Lattice Dynamics, Heat Capacities, and Debye-Waller Factors for Be and Zn Using a Modified Axially Symmetric Model

R. E. DeWames, T. Wolfram, and G. W. Lehman
North American Aviation Science Center, Thousand Oaks, California
(Received 20 August 1964; revised manuscript received 28 December 1964)

It is noted in this paper that the total energy of the electron-ion system in the metallic state arises from an electron self-energy term as well as volume-dependent pairwise interaction terms among the ions. The Slutsky-Garland model used by Schmunk *et al.* to analyze the experimental dispersion curves of Be does not give the proper elastic behavior. The experimental dispersion curves for beryllium and zinc measured by Schmunk *et al.* and Borgonovi *et al.*, respectively, are analyzed using a model consistent with the elastic behavior. For beryllium, the calculated dispersion curves agree well with the neutron inelastic-scattering data and the elastic constants of Smith and Arbogast. For zinc, the calculated frequencies are within the experimental uncertainties with the exception of the transverse branches along the $[0\bar{1}0]$ direction which describes atomic motions perpendicular to the basal planes. The experimental data on Zn indicate high dispersion and fluctuations in frequency ω *versus* wave number q. The calculated elastic constants agree within a few percent with the experimental data of Alers and Neighbours at 300°K, with the exception of C_{44} and C_{13}, which are low by 19% and 27%, respectively. The Debye-Waller factor and the specific heat for both metals are compared with available experimental data. It is found that the calculated specific heat for zinc is in excellent agreement with experiment over the whole temperature range. However, for beryllium, the calculated values are low for small temperatures; the discrepancy could be attributed to heavy impurities in beryllium. The anisotropy in the Debye-Waller factor for zinc is in good agreement with x-ray and Mössbauer experiments.

I. INTRODUCTION

THIS paper is concerned with the lattice dynamics, specific heat, and Debye-Waller factor for the hexagonal metals Be, Mg, and Zn. Our model is derived as a simple generalization of the A-S (axially symmetric) model.[1]

A general discussion of the nature of the dynamical forces arising in metals was presented at the Copenhagen conference.[2] In this paper, we point out that the correct form for the total energy E_T of a system of ions and electrons is a sum of two distinct terms

$$E_T = NE_0(a) + \tfrac{1}{2}\sum_{i\neq j}\sum V_\Gamma(R_{ij};a),$$

where $E_0(a)$ is an electron-gas self-energy term for a system containing N atoms, and $V_\Gamma(\mathbf{R}_{ij};a)$ denotes the potential energy of interaction between a pair of atoms separated by a distance $\mathbf{R}_{ij}$. Here, a represents the fact that both E_0 and V_Γ depend explicitly upon the volume of the atomic polyhedron. The subscript Γ denotes that V_Γ should transform according to the point group Γ at the center of the Brillouin zone associated with the metal in question. If one assumes that $V_\Gamma(\mathbf{R}_{ij};a) = V_0(|\mathbf{R}_{ij}|;a)$, the forces are central but volume-dependent. In previous papers on the lattice dynamics of Cu, Al, and β-Sn,[1-5] we chose the term axially symmetric, A-S, to represent the nature of this volume-dependent central force since two force constants arise per shell corresponding to a bond-stretching or radial force constant and an axially symmetric bond bending or tangential force constant.

The general features of the lattice dynamics of Be, Mg, and Zn using the A-S model have also been described recently.[2] However, it has proved difficult to achieve good elastic agreement in Be, β-Sn, and Zn with strictly A-S forces and we have been forced to introduce a slight modification of the A-S model, described later in this paper.

The lattice-dynamics models which have been compared with the experimental data of Schmunk *et al.* on Be[6] are the models of Begbie and Born[7] and of Slutsky and Garland,[8] the latter extended to include interactions with fourth- and fifth-nearest neighbors. These models give limited agreement with the data when the force constants in the models are evaluated from the neutron-scattering data. The Slutsky-Garland model for describing the dynamical motion of atoms in a hexagonal crystal is a restricted form of the A-S model[1] in which the tangent force constants or bond-bending force constants are set equal to zero. The reason Slutsky and Garland *a priori* set the tangent force constants equal to zero for every neighbor shell is not clear. However, if the explicit dependence of E_0 and $V_0(\mathbf{R}_{ij};a)$ upon a is dropped then $dE_T/da \equiv 0$ in the Slutsky-Garland model was required for the crystal to be in equilibrium. One should note that additional terms arise in dE_T/da owing to the electron gas com-

[1] G. W. Lehman, T. Wolfram, and R. E. DeWames, Phys. Rev. **128**, 1593 (1962).
[2] G. W. Lehman, T. Wolfram, and R. E. DeWames, J. Phys. Chem. Solids (to be published).
[3] T. Wolfram, G. W. Lehman, and R. E. DeWames, Phys. Rev. **129**, 2483 (1963).
[4] R. E. DeWames, T. Wolfram, and G. W. Lehman, Phys. Rev. **131**, 529 (1963).
[5] R. E. DeWames and G. W. Lehman, Phys. Rev. **135**, A170 (1964).
[6] R. E. Schmunk, R. M. Brugger, P. D. Randolph, and K. A. Strong, Phys. Rev. **128**, 562 (1962).
[7] G. H. Begbie and M. Born, Proc. Roy. Soc. (London) **A188**, 179 (1946).
[8] L. J. Slutsky and C. S. Garland, J. Chem. Phys. **26**, 787 (1957).

pressibility so that the A-S or volume-dependent central force model does not impose Cauchy-type relations.[2]

The previously mentioned restrictions introduced by Slutsky and Garland are so severe that one cannot obtain a fit to the dispersion curves of Be, Mg, or Zn which pass to the elastic limit correctly. In an attempt to correct the elastic inconsistency, Slutsky and Garland introduced, *a posteriori*, an electron-gas compressibility factor usually called σ. (This σ should not be confused with our σ_B defined later.) This procedure is completely unwarranted since their elastic limit is not derivable from the long-wavelength behavior of their dynamic equations.

Borgonovi *et al.*[9] measured the dispersion curves of zinc and analyzed their results using a tensor model including third- and fourth-nearest neighbors[10] with 13 independent interatomic force constants. Using these force constants one may calculate the five elastic constants implied by the model. Comparison of these predicted elastic constants with the experimental data of Alers and Neighbours[11] indicates that the dynamical matrix derived by Borgonovi *et al.* is inadequate in the long-wavelength region. In fact, Borgonovi *et al.* did not impose the elastic equations as constraints in the determination of the atomic force constants. A more serious omission is the failure to include fourth and fifth neighbors in their calculation. They used the dynamical matrix derived by Collins[10] for Mg and Be without taking note that the fourth-neighbor coordinates in the above two elements are the sixth-neighbor coordinates for Zn.

Recently Young and Koppel[12] using the force constants derived from the models discussed previously calculated the vibrational spectra and the specific heat. Because their resulting dynamical matrix is elastically inconsistent their calculation is inadequate in the long-wavelength region.

Our previous remarks indicate that the experimental data on Be and Zn have not been correctly analyzed to produce a consistent fit with the dispersion curves and elastic constants. Consequently, in Sec. II, the experimental data for beryllium and zinc are reanalyzed using a model based upon a modified A-S model derived with the assumption that the internal energy of the system can be written as a sum of bond-stretching and bond-bending terms, corresponding to restoring forces in the basal plane being different from those normal to the basal plane. The dynamical matrix associated with this modified A-S model is given in Appendix A. In Appendix B, we show the relationship between the modified A-S model and the general tensor force model derived by Collins in his study of Mg.[10] However, our study[2] as well as Iynegar's[13] indicates that the vibrational spectra and the elastic constants of Mg can be correlated quite well with a third-neighbor A-S model. The relation between the elastic constants and the atomic force constants is given in Sec. III. In Appendix C the constraints imposed by the A-S model on the elastic properties are presented and the need for modifying the axially symmetric nature of the model follows if the experimental data do not satisfy those constraints.

In Sec. IV the dynamical matrix is block-diagonalized along the principal directions in the Brillouin zone. The dispersion curves and the computed elastic constants are compared in Sec. V with the experimental data. The resulting Debye-Waller factor and the specific heat are also compared with the experimental data.

II. DYNAMICAL MATRIX IN THE CENTER-OF-MASS SYSTEM

Beryllium possesses the hexagonal close-packed structure which may be described as two interpenetrating simple hexagonal lattices. For convenience, the 0th atom of sublattice one is chosen as the origin, the first atom of the second sublattice is removed a distance

$$\mathbf{r}=\tfrac{1}{3}\mathbf{a}_1+\tfrac{2}{3}\mathbf{a}_2+\tfrac{1}{2}\mathbf{a}_3,$$

where $\mathbf{a}_1$, $\mathbf{a}_2$, and $\mathbf{a}_3$ are the primitive lattice basis vectors illustrated in Fig. 1. Also shown in this figure are the relative orientations of the Cartesian axes (x,y,z), hexagonal axes (a_1,a_2,a_3), and reciprocal lattice axes (b_1,b_2,b_3). The lattice parameters are $|a_1|=|a_2|=a=2.2856$ Å, $|a_3|=c=3.5832$ Å for beryllium, and $a=2.6648$ Å, $c=4.9467$ Å for zinc. The two inequivalent lattice sites give rise to six vibrational branches. In the long-wavelength limit three of these branches can be described as optical and three as acoustic. The following analysis is applicable to any crystal of hexagonal close-packed structure. The form of the dynamical matrix[1–5] is

$$\mathfrak{D}(\mathbf{q})=\begin{bmatrix}\mathbf{D}^{11}(\mathbf{q}) & \mathbf{D}^{12}(\mathbf{q})\\ \mathbf{D}^{12}(\mathbf{q})^* & \mathbf{D}^{11}(\mathbf{q})\end{bmatrix}. \tag{1}$$

Here, $\mathbf{q}$ denotes a vector in the first Brillouin zone and the elements, $\mathbf{D}^{\alpha\beta}(\mathbf{q})$ of the above 2×2 supermatrix are 3×3 matrices.

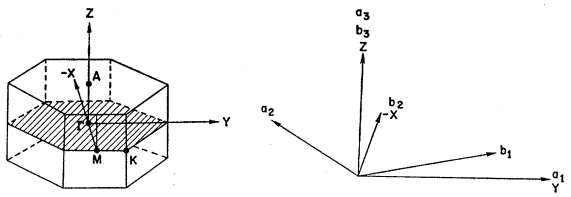

FIG. 1. First Brillouin zone of the hexagonal lattice. Also shown are the basis vectors of the hexagonal lattice (a's) the reciprocal basis vectors (b's) and the Cartesian-system basis vectors (x's).

[9] G. Borgonovi, G. Caglioti, and J. J. Antel, Phys. Rev. **132**, 683 (1963).
[10] M. F. Collins, Proc. Phys. Soc. (London) **80**, 362 (1962).
[11] G. A. Alers and J. R. Neighbours, J. Phys. Chem. Solids **7**, 58 (1958).
[12] James A. Young and Juan U. Koppel, Phys. Rev. **134**, A1476 (1964).
[13] P. K. Iyengar, J. Phys. Chem. Solids (to be published).

The elements of Eq. (1) are derived in Appendix A. $\mathfrak{D}(\mathbf{q})$ can be transformed to a real form by the unitary transformation

$$\mathbf{u}=\frac{1}{\sqrt{2}}\begin{bmatrix}\mathbf{I} & -\mathbf{I}i\\ -\mathbf{I}i & \mathbf{I}\end{bmatrix},$$

where $\mathbf{I}$ is a 3×3 unit matrix and i the square root of -1. For the transformed dynamical matrix $\mathbf{L}(\mathbf{q})$, we obtain

$$\mathbf{L}(\mathbf{q})=\mathbf{u}^*\mathfrak{D}(\mathbf{q})\mathbf{u}=\begin{bmatrix}\mathbf{D}^{11}+\mathrm{Im}\mathbf{D}^{12} & \mathrm{Re}\mathbf{D}^{12}\\ \mathrm{Re}\mathbf{D}^{12} & \mathbf{D}^{11}-\mathrm{Im}\mathbf{D}^{12}\end{bmatrix},$$

where $\mathrm{Re}\mathbf{D}^{12}$ and $\mathrm{Im}\mathbf{D}^{12}$ denote the real and imaginary parts of the matrix $\mathbf{D}^{12}$. Now by means of the unitary super matrix $\mathbf{V}$,

$$\mathbf{V}=\frac{1}{\sqrt{2}}\begin{bmatrix}\mathbf{I} & -\mathbf{I}\\ \mathbf{I} & \mathbf{I}\end{bmatrix},$$

the dynamical matrix can be transformed to the center-of-mass system where it is

$$\mathbf{\Lambda}(\mathbf{q})=\mathbf{V}^*\mathbf{L}(\mathbf{q})\mathbf{V}=\begin{bmatrix}\mathbf{D}^{11}+\mathrm{Re}\mathbf{D}^{12} & -\mathrm{Im}\mathbf{D}^{12}\\ -\mathrm{Im}\mathbf{D}^{12} & \mathbf{D}^{11}-\mathrm{Re}\mathbf{D}^{12}\end{bmatrix}. \quad (2)$$

$\mathbf{\Lambda}(\mathbf{0})$ is block-diagonal since $\mathrm{Im}\mathbf{D}^{12}(\mathbf{q}=0)=0$. Furthermore, it can be shown that $\mathbf{D}^{11}(\mathbf{0})=-\mathrm{Re}\mathbf{D}^{12}(\mathbf{0})$. The matrix $\mathbf{D}^{11}+\mathrm{Re}\mathbf{D}^{12}-\mathrm{Im}\mathbf{D}^{12}\{\mathbf{D}^{11}-\mathrm{Re}\mathbf{D}^{12}\}^{-1}\mathrm{Im}\mathbf{D}^{12}$ corresponds to the acoustic matrix in the long-wavelength limit. The optical frequencies for small propagation vectors are determined by the matrix $\mathbf{D}^{11}-\mathrm{Re}\mathbf{D}^{12}$. The three optical frequencies at the center of the Brillouin zone consist of a twofold degenerate root ω_a and a single frequency ω_b.

It is easily shown from the dynamical matrix elements given in Appendix A that

$$\mathbf{D}^{11}-\mathrm{Re}\mathbf{D}^{12}=2\mathbf{D}^{11}(\mathbf{0})=\begin{bmatrix}\omega_a^2 & 0 & 0\\ 0 & \omega_a^2 & 0\\ 0 & 0 & \omega_b^2\end{bmatrix},$$

where

$$\omega_a^2=(12/m)\{\epsilon_{1x}+\epsilon_{3x}+2\epsilon_{5x}+2\delta_1+8\delta_3+28\delta_5\} \quad (3)$$

and

$$\omega_b^2=(12/m)\{(\epsilon_{1z}+\epsilon_{3z}+2\epsilon_{5z})+3\gamma^2(\delta_1+\delta_3+2\delta_5)\}. \quad (4)$$

The parameters are force constants defined in Appendix A, and m denotes the atomic mass.

III. ELASTIC EQUATIONS AND ATOMIC FORCE CONSTANTS

The dynamical matrix, $\mathbf{E}(\mathbf{q})$, for the acoustic modes of a crystal with hexagonal symmetry is given in Appendix C. The frequencies are determined by the secular equation

$$|\mathbf{E}(\mathbf{q})-\omega^2\mathbf{I}|=0. \quad (5)$$

Along the [100] direction, the transverse acoustic (TA) and longitudinal acoustic (LA) frequencies are

$$\begin{aligned}&\rho(\omega_{\mathrm{TA}2})^2=C_{44}q^2,\\ &\rho(\omega_{\mathrm{TA}1})^2=\tfrac{1}{2}(C_{11}-C_{12})q^2,\\ &\rho(\omega_{\mathrm{LA}})^2=C_{11}q^2.\end{aligned} \quad (6)$$

The frequencies for elastic waves propagating along the [001] direction are

$$\begin{aligned}&\rho(\omega_{\mathrm{TA}})^2=C_{44}q^2,\\ &\rho(\omega_{\mathrm{TA}})^2=C_{44}q^2,\\ &\rho(\omega_{\mathrm{LA}})^2=C_{33}q^2.\end{aligned} \quad (7)$$

The atomic force constants may be related to the elastic constants by equating the elements of $\mathbf{\Lambda}(\mathbf{q})$ to those of the dynamical matrix of elasticity theory, Eq. (C.3), in the long-wavelength limit. Using the modified A-S model (see Appendix A), we obtained the following independent equations relating the atomic force constants to the elastic constants:

$$\begin{aligned}
C_{11}&=\frac{4}{c\sqrt{3}}\left\{(9/8)\alpha_2+(27/8)\alpha_6+\tfrac{3}{2}\delta_1+24\delta_3+147\delta_5+\tfrac{3}{2}\beta_{2x}+\tfrac{9}{2}\beta_{6x}+\tfrac{1}{2}\epsilon_{1x}+2\epsilon_{3x}+7\epsilon_{5x}-\frac{12}{m\omega_a^2}(8\delta_3-\delta_1-20\delta_5)^2\right\},\\
C_{11}-C_{12}&=\frac{8}{c\sqrt{3}}\left\{\tfrac{3}{8}\alpha_2+(9/8)\alpha_6+\tfrac{1}{2}\delta_1+8\delta_3+49\delta_5+\tfrac{3}{2}\beta_{2x}+\tfrac{9}{2}\beta_{6x}+\tfrac{1}{2}\epsilon_{1x}+2\epsilon_{3x}+7\epsilon_{5x}-\frac{12}{m\omega_a^2}(8\delta_3-\delta_1-20\delta_5)^2\right\},\\
C_{44}&=\frac{4\gamma^2}{c\sqrt{3}}\{\tfrac{3}{2}\delta_1+6\delta_3+21\delta_5+\beta_{4x}+\tfrac{3}{4}\epsilon_{1x}+\tfrac{3}{4}\epsilon_{3x}+\tfrac{3}{2}\epsilon_{5x}\},\\
C_{12}+C_{11}&=\frac{8}{c\sqrt{3}}\{\tfrac{3}{4}\alpha_2+(9/4)\alpha_6+\delta_1+16\delta_3+98\delta_5\},\\
(C_{13}+C_{44})&=\frac{4\gamma^2}{c\sqrt{3}}\{3\delta_1+12\delta_3+42\delta_5\},\\
C_{44}&=\frac{4}{c\sqrt{3}}\{\tfrac{3}{2}\gamma^2\delta_1+6\gamma^2\delta_3+21\gamma^2\delta_5+\tfrac{3}{2}\beta_{2z}+\tfrac{9}{2}\beta_{6z}+\tfrac{1}{2}\epsilon_{1z}+2\epsilon_{3z}+7\epsilon_{5z}\},\\
C_{33}&=\frac{4\gamma^2}{c\sqrt{3}}\{\alpha_4+(9/4)\gamma^2\delta_1+(9/4)\gamma^2\delta_3+\tfrac{9}{2}\gamma^2\delta_5+\beta_{4z}+\tfrac{3}{4}\epsilon_{1z}+\tfrac{3}{4}\epsilon_{3z}+\tfrac{3}{2}\epsilon_{5z}\},
\end{aligned} \quad (8)$$

where the parameters are force constants defined in Appendix A. Using the above relations we obtain

$$c\sqrt{3}(C_{44}-C_{13})=8\gamma^2\{\beta_{4x}+\tfrac{3}{4}\epsilon_{1x}+\tfrac{3}{4}\epsilon_{3x}+\tfrac{3}{2}\epsilon_{5x}\}.$$

Hence, if the atomic force constants β and ϵ (bond-bending) are not included in the model, the Cauchy relation $C_{13}=C_{44}$ is obtained. Another useful relation connecting C_{13} and C_{44} is given by

$$c\sqrt{3}(C_{44}-C_{13})=8\{\tfrac{3}{2}\beta_{2z}+\tfrac{9}{2}\beta_{6z}+\tfrac{1}{2}\epsilon_{1z}+2\epsilon_{3z}+7\epsilon_{5z}\}.$$

Similarly it can be shown that

$$(c\sqrt{3}/16)(3C_{12}-C_{11})$$
$$=-[\tfrac{3}{2}\beta_{2x}+\tfrac{9}{2}\beta_{6x}+\tfrac{1}{2}\epsilon_{1x}+2\epsilon_{3x}+7\epsilon_{5x}]$$
$$+(12/m\omega_a^2)(8\delta_3-\delta_1-20\delta_5)^2,$$

which gives the other Cauchy relation that $3C_{12}-C_{11}=0$ if the bond-bending and the second term (optical correction to the acoustical matrix) are neglected. From the experimental elastic data the left-hand side of the above equation is negative and consequently cannot be equated to the optical correction alone since it is positive definite.

The A-S model requires that the constants with subscript x be equal to those with subscript z. Under those conditions it follows from the above equations that

$$(c\sqrt{3}/16)[3C_{12}-C_{11}+2C_{44}-2C_{13}]$$
$$=(12/m\omega_a^2)(8\delta_3-\delta_1-20\delta_5)^2. \quad (9)$$

The available elastic data show that the above constraint is not desirable except for magnesium. However, in the case of beryllium it is possible to fit the experimental data with the constraint that the bond-bending constants with the z subscripts be proportional to those with the x subscripts with the constant of proportionality σ_B the same for all neighbors.

Under these conditions we obtain

$$(c\sqrt{3}/16)[3C_{12}-C_{11}+2\sigma_B^{-1}(C_{44}-C_{13})]$$
$$=(12/m\omega_a^2)(8\delta_3-\delta_1-20\delta_5)^2. \quad (10)$$

The value of σ_B for beryllium is obtained by solving the above equation self-consistently. It is first assumed that the optical correction is zero; this allows calculation of σ_B. Using special points in the Brillouin zone and the elastic constraints the atomic force constants can then be calculated and the optical correction evaluated and inserted in Eq. (10). This gives a new value of σ_B. The calculation is then repeated until self-consistency is achieved. Results of calculations are summarized in Sec. V.

IV. BLOCK DIAGONALIZATION OF THE DYNAMICAL MATRIX $\mathbf{A}(q)$ ALONG PRINCIPAL DIRECTIONS

Using group-theoretical arguments, one can block diagonalize the dynamical matrix along the principal symmetry directions. Along the direction in the Brillouin zone the block diagonalized [0001] dynamical matrix is given by

$$\mathbf{A}[\mathbf{q}=(0,0,q_z)]$$
$$=\begin{bmatrix} D_{xx}^{11}+\mathrm{Re}D_{xx}^{12} & 0 & 0 & 0 & 0 & 0 \\ 0 & D_{xx}^{11}+\mathrm{Re}D_{xx}^{12} & 0 & 0 & 0 & 0 \\ 0 & 0 & D_{zz}^{11}+\mathrm{Re}D_{zz}^{12} & 0 & 0 & 0 \\ 0 & 0 & 0 & D_{xx}^{11}-\mathrm{Re}D_{xx}^{12} & 0 & 0 \\ 0 & 0 & 0 & 0 & D_{xx}^{11}-\mathrm{Re}D_{xx}^{12} & 0 \\ 0 & 0 & 0 & 0 & 0 & D_{zz}^{11}-\mathrm{Re}D_{zz}^{12} \end{bmatrix}. \quad (11)$$

The acoustic frequencies are

$$(\omega_{\mathrm{TA}})^2=\frac{\omega_a^2}{2}(1-C_z)+\left(\frac{2\beta_{4x}}{m}\right)(1-C_{2z}), \quad (12)$$

$$(\omega_{\mathrm{LA}})^2=\left(\frac{\omega_b^2}{2}\right)(1-C_z)+\frac{2(\alpha_4+\beta_{4z})}{m}(1-C_{2z}). \quad (13)$$

The transverse optic (TO) and longitudinal optic (LO) frequencies are

$$(\omega_{\mathrm{TO}})^2=(\tfrac{1}{2}\omega_a^2)(1+C_z)+(2\beta_{4x}/m)(1-C_{2z}), \quad (14)$$

$$(\omega_{\mathrm{LO}})^2=(\tfrac{1}{2}\omega_b^2)(1+C_z)+(2(\alpha_4+\beta_{4z})/m)(1-C_{2z}). \quad (15)$$

From the above equations it follows that

$$(\omega_{\mathrm{TO}})^2\left[\mathbf{q}=\left(0,0,\frac{\pi}{c}\right)\right]=(\omega_{\mathrm{TA}})^2\left[\mathbf{q}=\left(0,0,\frac{\pi}{c}\right)\right]=\frac{\omega_a^2}{2}+\frac{4\beta_{4x}}{m}, \quad (16)$$

$$(\omega_{\mathrm{LO}})^2\left[\mathbf{q}=\left(0,0,\frac{\pi}{c}\right)\right]=(\omega_{\mathrm{LA}})^2\left[\mathbf{q}=\left(0,0,\frac{\pi}{c}\right)\right]=\frac{\omega_b^2}{2}+\frac{4\alpha_4+4\beta_{4z}}{m}. \quad (17)$$

Using the elastic equations it can be shown that

$$\omega_a^2=(4/m)\{\gamma^{-2}c\sqrt{3}C_{44}-4\beta_{4x}\}, \tag{18}$$

$$\omega_b^2=(4/m)\{\gamma^{-2}c\sqrt{3}C_{33}-4\beta_{4z}-4\alpha_4\}. \tag{19}$$

If the fourth-neighbor atomic force constants for beryllium or the sixth neighbors for zinc are neglected the elastic properties determine the dispersion curves along [0,0,0,1].

For the elastic waves propagating along the $[01\bar{1}0]$ direction

$$\Lambda=\mathbf{q}=(q_x0,0)$$

$$=\begin{bmatrix} D_{xx}^{11}+\mathrm{Re}D_{xx}^{12} & -\mathrm{Im}D_{xx}^{12} & 0 & 0 & 0 & 0 \\ -\mathrm{Im}D_{xx}^{12} & D_{xx}^{11}-\mathrm{Re}D_{xx}^{12} & 0 & 0 & 0 & 0 \\ 0 & 0 & D_{yy}^{11}+\mathrm{Re}D_{yy}^{12} & -\mathrm{Im}D_{yy}^{12} & 0 & 0 \\ 0 & 0 & -\mathrm{Im}D_{yy}^{12} & D_{yy}^{11}-\mathrm{Re}D_{yy}^{12} & 0 & 0 \\ 0 & 0 & 0 & 0 & D_{zz}^{11}+\mathrm{Re}D_{zz}^{12} & -\mathrm{Im}D_{zz}^{12} \\ 0 & 0 & 0 & 0 & -\mathrm{Im}D_{zz}^{12} & D_{zz}^{11}-\mathrm{Re}D_{zz}^{12} \end{bmatrix}. \tag{20}$$

Hence, the dynamical matrix breaks up into three 2×2 matrices. At the end of the zone $\mathbf{q}=(2\pi/\sqrt{3}a,0,0)$ it can be shown that

$$\mathrm{Im}D_{xx}^{12}=\sqrt{3}\,\mathrm{Re}D_{xx}^{12},\quad \mathrm{Im}D_{yy}^{12}=\sqrt{3}\,\mathrm{Re}D_{yy}^{12},\quad \mathrm{Im}D_{zz}^{12}=\sqrt{3}\,\mathrm{Re}D_{zz}^{12}. \tag{21}$$

The frequencies are

$$(\omega_{\mathrm{LO}})^2=D_{xx}^{11}+2\,\mathrm{Re}D_{xx}^{12}=\frac{1}{m}\{16\delta_1+4\epsilon_{1x}+96\delta_3+12\epsilon_{3x}+128\delta_5+8\epsilon_{5x}+6\alpha_2+8\beta_{2x}+2\alpha_6+8\beta_{6x}\}, \tag{22}$$

$$(\omega_{\mathrm{LA}})^2=D_{xx}^{11}-2\,\mathrm{Re}D_{xx}^{12}=\frac{1}{m}\{8\delta_1+8\epsilon_{1x}+208\delta_5+16\epsilon_{5x}+6\alpha_2+8\beta_{2x}+2\alpha_6+8\beta_{6x}\}, \tag{23}$$

$$(\omega_{\mathrm{TO1}})^2=D_{yy}^{11}+2\,\mathrm{Re}D_{yy}^{12}=\frac{1}{m}\{24\delta_1+8\epsilon_{1x}+240\delta_5+16\epsilon_{5x}+2\alpha_2+8\beta_{2x}+6\alpha_6+8\beta_{6x}\}, \tag{24}$$

$$(\omega_{\mathrm{TA1}})^2=D_{yy}^{11}-2\,\mathrm{Re}D_{yy}^{12}=\frac{1}{m}\{4\epsilon_{1x}+96\delta_3+12\epsilon_{3x}+96\delta_5+8\epsilon_{5x}+2\alpha_2+8\beta_{2x}+6\alpha_6+8\beta_{6x}\}, \tag{25}$$

$$(\omega_{\mathrm{TA2}})^2=D_{zz}^{11}-2\,\mathrm{Re}D_{zz}^{12}=\frac{1}{m}\{12\gamma^2\delta_1+36\gamma^2\delta_3+24\gamma^2\delta_5+4\epsilon_{1z}+12\epsilon_{3z}+8\epsilon_{5z}+8\beta_{2z}+8\beta_{6z}\}, \tag{26}$$

$$(\omega_{\mathrm{TO2}})^2=D_{zz}^{11}+2\,\mathrm{Re}D_{zz}^{12}=\frac{1}{m}\{24\gamma^2\delta_1+48\gamma^2\delta_5+8\epsilon_{1z}+16\epsilon_{5z}+8\beta_{2z}+8\beta_{6z}\}. \tag{27}$$

Along the $[11\bar{2}0]$ direction

$$\Lambda[\mathbf{q}=(0,q_y,0)]$$

$$=\begin{bmatrix} D_{xx}^{11}+\mathrm{Re}D_{xx}^{12} & -\mathrm{Im}D_{xy}^{12} & 0 & 0 & 0 & 0 \\ -\mathrm{Im}D_{xy}^{12} & D_{yy}^{11}-\mathrm{Re}D_{yy}^{12} & 0 & 0 & 0 & 0 \\ 0 & 0 & D_{yy}^{11}+\mathrm{Re}D_{yy}^{12} & -\mathrm{Im}D_{xy}^{12} & 0 & 0 \\ 0 & 0 & -\mathrm{Im}D_{xy}^{12} & D_{xx}^{11}-\mathrm{Re}D_{xx}^{12} & 0 & 0 \\ 0 & 0 & 0 & 0 & D_{zz}^{11}+\mathrm{Re}D_{zz}^{12} & 0 \\ 0 & 0 & 0 & 0 & 0 & D_{zz}^{11}-\mathrm{Re}D_{zz}^{12} \end{bmatrix}. \tag{28}$$

At the end of the zone the frequencies are

$$(\omega_{\mathrm{LO}})^2=(\omega_{\mathrm{LA}})^2=\tfrac{1}{2}\omega_a^2+(9/2m)[\alpha_2+2\beta_{2x}], \tag{29}$$

$$(\omega_{\mathrm{TO1}})^2=\tfrac{1}{2}\omega_a^2+(1/m)[\tfrac{1}{2}9\alpha_2+9\beta_{2x}+12\delta_1+48\delta_3-156\delta_5], \tag{30}$$

$$(\omega_{\mathrm{TA1}})^2=\tfrac{1}{2}\omega_a^2+(1/m)[\tfrac{1}{2}9\alpha_2+9\beta_{2x}-12\delta_1-48\delta_3+156\delta_5], \tag{31}$$

$$(\omega_{\mathrm{TO2}})^2=(\omega_{\mathrm{TA2}})^2=\tfrac{1}{2}\omega_b^2+9\beta_{2z}/m. \tag{32}$$

V. NUMERICAL RESULTS AND DISCUSSIONS

Beryllium

A. Dispersion Curves

Table I gives the atomic force constants for the modified A-S model. Using these atomic force constants we calculated the elastic constants. The results are summarized in Table II together with the experimentally determined elastic constants[14] and the elastic

[14] J. F. Smith and C. L. Arbogast, J. Appl. Phys. **31**, 99 (1960).

TABLE I. Atomic force constants for beryllium (in units of 10^4 dyn/cm).

$K(1,12)=2.215$	$K(3,12)=1.199$	$K(5,12)=-0.0690$
$C_{Bx}(1,12)=0.1383$	$C_{Bx}(3,12)=-0.2671$	$C_{Bx}(5,12)=0.1500$
$K(2,11)=1.357$	$K(4,11)=0.2039$	$K(6,11)=0.309$
$C_{Bx}(2,11)=0.0756$	$C_{Bx}(4,11)=0.3225$	$C_{Bx}(6,11)=0.0335$
	$\sigma_B=1.306$	

constants derived from a SG (Slutsky and Garland) model[8] used by Schmunk *et al.*[6] to fit the neutron inelastic data. Clearly, the SG model is inadequate to

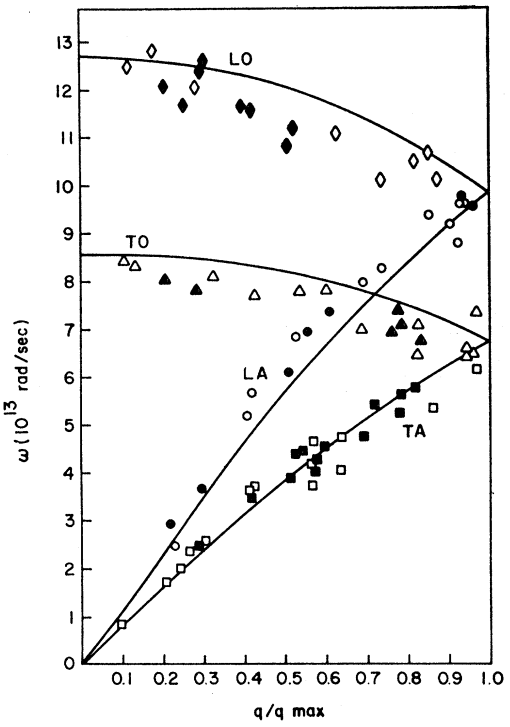

FIG. 2. Calculated and measured dispersion curves along the [0001] direction for beryllium.

represent the lattice of dynamics of beryllium since the dynamical matrix is inconsistent with the elastic matrix. Introducing the bulk compressibility σ of the

TABLE II. Comparison of calculated and experimental elastic constants for beryllium (in units of 10^{11} dyn/cm^2).

Elastic constants	Experiment[a]	Slutsky-Garland model Not using σ	Slutsky-Garland model Using σ	Axially symmetric model (modified)
C_{11}	29.94	25.95	10.43	29.55
C_{33}	34.22	34.0	18.48	33.77
C_{44}	16.62	10.6	10.6	16.00
C_{12}	2.76±0.08	10.4	−5.12	3.16
C_{13}	1.1 ±0.5	10.6	−4.92	1.74
$\sigma=C_{13}-C_{44}=-15.52$			−15.52	···

[a] See Ref. 13.

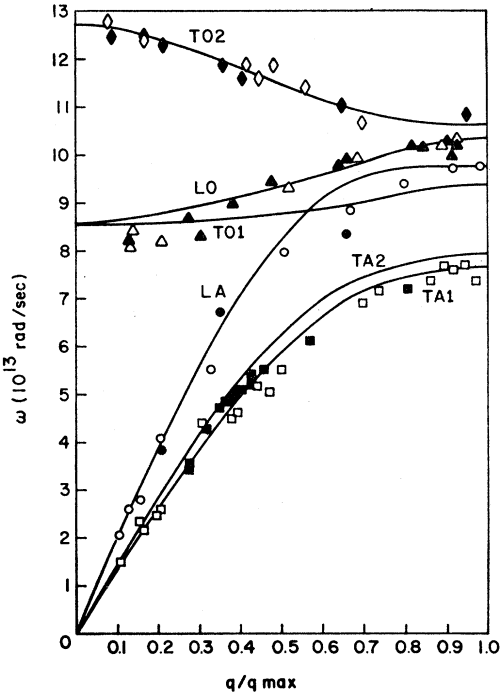

FIG. 3. Calculated and measured dispersion curves along the [01$\bar{1}$0] direction for beryllium.

electron gas as a measure of the deviation from the Cauchy relation is inconsistent with the SG fit to the dispersion curves and gives unrealistic elastic constants.

The dispersion curves calculated from the atomic force constants given in Table I are shown in Figs. 2–4, where they are compared with the experimental data. The agreement with experiment is obviously quite good.

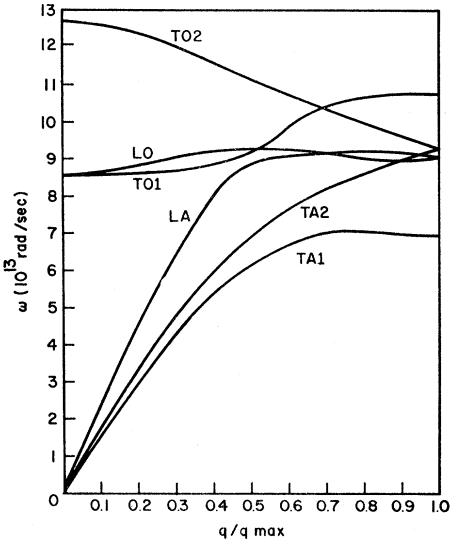

FIG. 4. Calculated dispersion curves along the [11$\bar{2}$0] direction for beryllium.

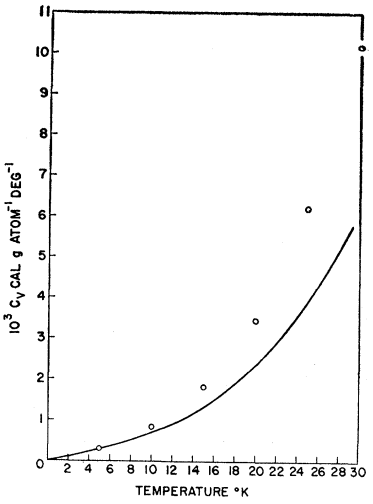

FIG. 5. Calculated and measured heat capacity of beryllium from 0–30°K.

The curves labeled TA1, TA2 refer to modes of vibrations polarized in the basal plane and normal to the basal plane, respectively. TA1 and TO1 were not measured by Schmunk *et al.* nor were the dispersion curves along the [11$\bar{2}$0] direction. In order to calculate the transverse modes polarized in the basal plane use is made of the present elastic data where the value of C_{12} plays an important role in determining the slopes of the above branches. Hence, it would be interesting to investigate these polarizations experimentally.

B. Specific Heat

Since the dynamical matrix for the modified A-S model gives good agreement with the dispersion curves and is elastically consistent, it is interesting to compare the calculated specific heat with the present experimental data. The results are shown in Figs. 5–7. In the calculation the electronic contribution is added to the lattice contribution with $\gamma=5.4\times10^{-5}$. Below 80°K C_v (calculated) is low compared with the experimental data of Hill and Smith[15]; consequently, the Debye characteristic temperature θ would be higher than that obtained from the specific heat data. Alers and Neighbours[11] calculated θ from the elastic data of Smith and Arbogast[14] and came to a similar conclusion. An explanation of this discrepancy could arise from large quasilocalized phonon mode contributions to C_v due to heavy impurities in the Be samples.

If one uses the dynamical matrix for the SG model which gives lower elastic constants, the resulting specific heat would be higher and perhaps closer to the experimental values. However, such agreement would certainly be fortuitous.[12]

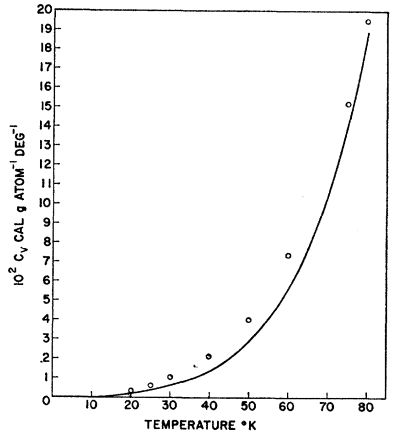

FIG. 6. Calculated and measured heat capacity of beryllium from 0–80°K.

[15] R. W. Hill and P. L. Smith, Phil. Mag. 44, 636 (1953).

C. The Debye-Waller Factor

The only available experimental data which gives information about the mean square displacement of the Be atom in the Be lattice is that obtained through Mössbauer experiments with Fe^{57} in Be.[16,17] If the impurity goes in the host lattice substitutionally and isotopically it can be shown[18] that the mean-square displacement of the impurity becomes equal to the mean-square displacement of the host at *high temperatures*. Furthermore, at $T=0$ it can be shown that under the above conditions using a Debye model that

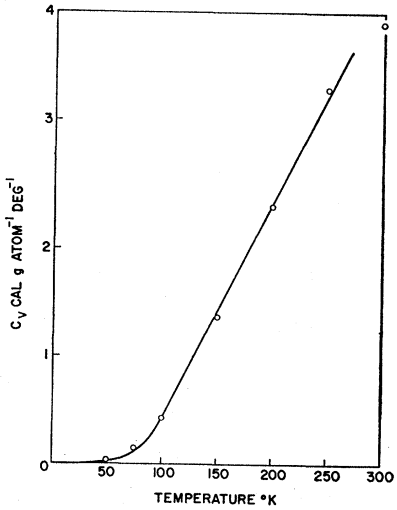

FIG. 7. Calculated and measured heat capacity of beryllium from 0–300°K.

$$\frac{\langle x^2\rangle_{\text{imp}}}{\langle x^2\rangle_{\text{host}}}=\frac{2}{\sqrt{3}}\left(\frac{1}{\epsilon}\right)^{1/2}, \tag{33}$$

where

$$\epsilon=(M_I-M_H)/M_H \quad \text{and} \quad M_I\gg M_H.$$

These relations make it desirable to compare our

[16] R. M. Housley, N. E. Erickson, and J. G. Dash (to be published).

[17] J. P. Schiffer, P. N. Parks, and Juergen Heberle, Phys. Rev. 133, 1553 (1964).

[18] G. W. Lehman and R. E. DeWames, Phys. Rev. 131, 1008 (1963).

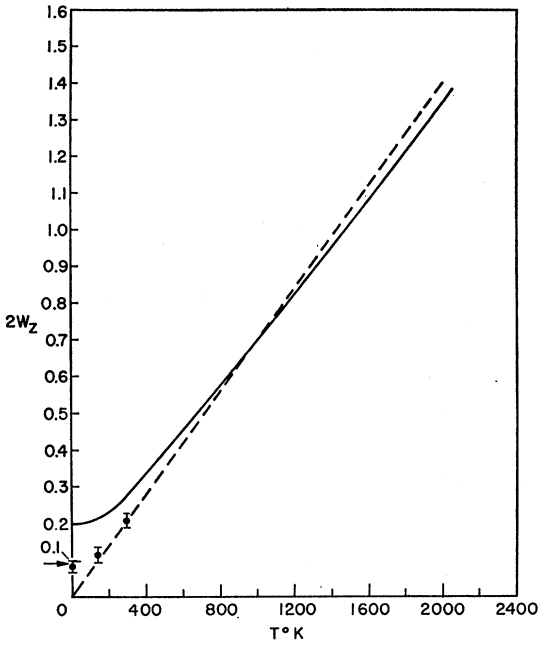

FIG. 8. The full line represents the mean-square displacement for beryllium. The dashed line is an extrapolation of the measured Debye-Waller factor of Fe^{57} in Be determined by Mössbauer experiments. The full dots are the measured values.

theoretical results with the Mössbauer experiment of Fe^{57} in Be. In the calculation of $2W$, the transition energy of the emitting or absorbing particle is taken to be that of the Fe^{57} nucleus. The results are shown in Fig. 8. The full curve represents $2W$ for the host crystal. The experimental results of Housley *et al.*[16] and Schiffer *et al.*[17] are indicated by full and open circles, respectively. The dotted line represents a linear extrapolation of the experimental value at 297°K. The arrow represents the calculated value of $2W$ using Eq. (33). Clearly within the experimental uncertainties one can conclude from Fig. 8 that the mean-square displacement of Fe^{57} in Be can be adequately described by considering only a mass change. The anisotropy factor, $\epsilon=2W_{xx}/2W_{zz}$ varies from 1.08–1.15 between 4 and 2000°K. Housley *et al.* found the Debye-Waller f to be about 1% smaller parallel to than perpendicular to the c axis with an experimental uncertainty of about 1%.

Zinc

A. Dispersion Curves

Table III gives the atomic force constants for the modified A-S model. Using these atomic force constants we calculated the elastic constants which are summarized in Table IV together with the experimentally determined elastic[11] constants and the elastic constants resulting from a fourth-neighbor tensor model fit to the neutron inelastic data.[9,10] The modified A-S constants give very good agreement with the elastic data

TABLE III. Atomic force constants for zinc (in units of 10^4 dyn/cm).

$K(1,11)=2.665$	$K(2,12)=0.8258$	$K(3,12)=0.4164$
$C_{Bx}(1,11)=-0.0978$	$C_{Bx}(2,12)=-0.1027$	$C_{Bx}(3,12)=-0.0688$
$C_{Bz}(1,11)=-0.3473$	$C_{Bz}(2,12)=-0.0893$	$C_{Bz}(3,12)=-0.0241$
$K(4,11)=-0.1972$	$K(5,12)=0.0667$	$K(6,11)+C_{Bz}(6,11)$
$C_{Bx}(4,11)=0.0841$	$C_{Bx}(5,12)=0.0293$	$=-0.1484$
$C_{Bz}(4,11)=0.0583$	$C_{Bz}(5,12)=0.03905$	$C_{Bx}(6,11)=0.0624$

with the exception of C_{44} and C_{13}. The fourth-neighbor tensor fit obviously is elastically inconsistent. Furthermore, the fit of the [0001]T branch does not give C_{44} consistent with the fit of the [0110]TA2 branch which is required from the elastic properties.

TABLE IV. Comparison of calculated and experimental elastic constants for zinc (in units of 10^{11} dyn/cm^2).

Elastic constants	Experiment 4°K	Experiment 295°K	Fourth-neighbor tensor model	Axially symmetric model (modified)
C_{11}	17.909	16.368	14.43	15.39
C_{33}	6.88	6.347	4.63	6.78
C_{44}	4.595	3.879	1.63	3.15
C_{12}	3.75	3.64	5.39	3.62
C_{13}	5.54	5.30	···	3.85

The dispersion curves calculated from the atomic force constants in Table III are shown in Fig. 9–11, where they are compared with the experimental data.

The agreement in general is quite good. In order to get a representative fit of TA2 along the [01$\bar{1}$0] it was necessary to decrease C_{44}; this had the effect of giving low values for TA along the [0001] branch. Definitely, the experimental values for TA2 show anomalous behavior; however, we feel that the A-S modified model is adequate for the purpose of evaluating the dynamical and thermal properties of zinc, Table IV. The full

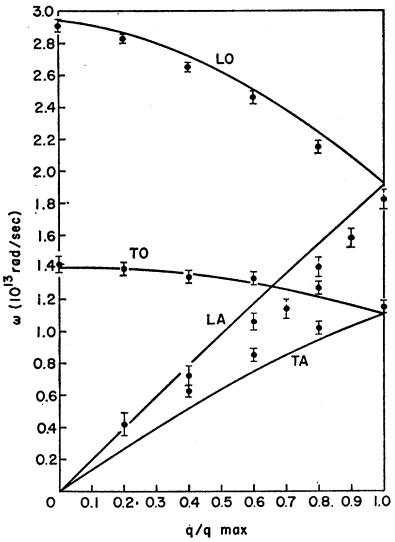

FIG. 9. Calculated and measured dispersion curves along the [0001] direction for zinc.

tensor fit to the dispersion curves is on the average comparable with the A-S modified model. Since the elastic data of zinc is strongly temperature-dependent, zinc is a good candidate for studying dispersion curves as a function of temperature.

B. Specific Heat

In Fig. 12 the calculated specific heat is compared with the experimental data. The fit is very good over the whole temperature range. This agreement for zinc could further support the previous conjecture that in beryllium the deviation from the calculated values is due to the impurities. From previous calculations and from experiment[19] on Mg-Pb and Mg-Cd systems it is known that small amounts of heavy impurities cause large effects in the specific heat of light elements.

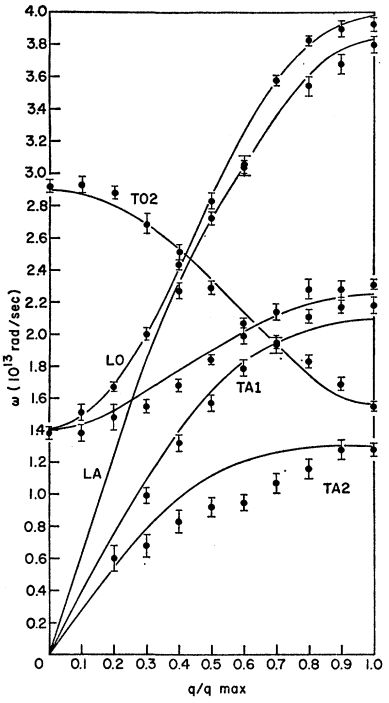

FIG. 10. Calculated and measured dispersion curves along the [0110] direction for zinc.

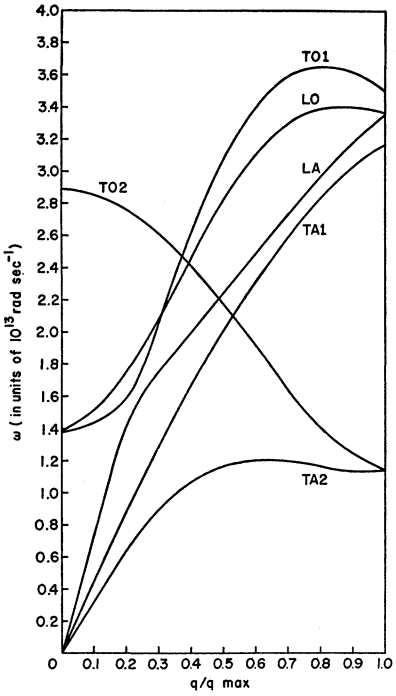

FIG. 11. Calculated and measured dispersion curves along the [11$\bar{2}$0] direction for zinc.

C. Debye-Waller Factor

In Table V we listed the quantity $H_{zz}(T)$ and the anisotropy factor $\epsilon(T)$ which are necessary to calculate $2W$ for all orientations of the crystal.[5] In Table VI comparison is made with the earlier work of Zener[20] and the x-ray determination of $2W$ of Brindley[21] and of Jauncey and Bruce.[22] The calculated anisotropy is in good agreement with the x-ray data; however, the magnitude of H_{zz} is quite different. Using the results of Table V we obtained $f_{xx}=0.013$ and $f_{zz}=0.00034$ at 4°K with a recoil energy $R=6.9\times10^{-2}$ eV. Hence, it should be possible to measure f for zinc at 4°K. For

TABLE V. Temperature dependence of $H_{zz}(T)$ and $\epsilon(T)$ for zinc.

T°K	$H_{zz}(T)$ (10^3 eV^{-1})	$\epsilon(T)$
4	0.115	0.55
50	0.162	0.46
100	0.271	0.39
200	0.514	0.36
298	0.758	0.35

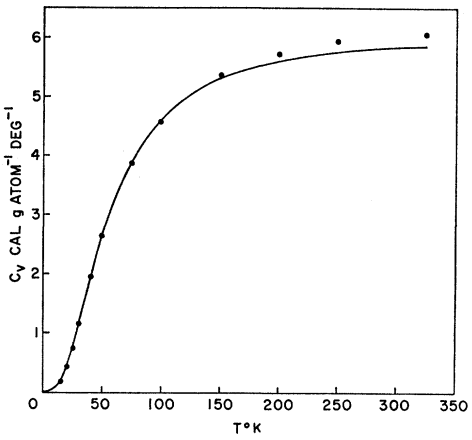

FIG. 12. Calculated and measured heat capacity of zinc from 0–350°K.

[19] G. W. Lehman, J. A. Cape, R. E. DeWames and D. H. Leslie, Bull. Am. Phys. Soc. **9**, 251 (1964).

[20] C. Zener and S. Bilinsky, Phys. Rev. **50**, 489 (1936).

[21] G. W. Brindley, Phil. Mag. **21**, 790 (1936).

[22] G. E. M. Jauncey and W. A. Bruce, Phys. Rev. **50**, 408 (1936).

TABLE VI. Comparison of $H_{zz}(T)$ with earlier work at 298°K (10^3 eV^{-1}).

	H_{zz}	ϵ
Simple Debye model	0.59	0.56
Brindley	1.02	0.394
Jauncey and Bruce	1.85	0.29
Modified Debye model	0.84	0.56
Present calculation	0.758	0.35

comparison if one takes a θ_D (specific heat) of 320°K then one obtains $f_D=0.0247$ at 0°K.

Recently Housley *et al.*[23] measured the anisotropy in f by diffusing Co^{57} in a Zn single crystal. At room temperature they found $\langle x^2\rangle$ parallel to the c axis about twice the perpendicular value. The measured $\langle x^2\rangle$ at room temperature is about 20% smaller than the calculated value. Similarly, Kundig *et al.*[24] measured f in a polycrystal source of Co^{57} in Zn between 120 and 380°K. The intensity of the two quadrupole split lines decreases with temperature

$$[A=(I(120°\text{K})-I(380°\text{K}))/I(120°\text{K})=42\pm3\%].$$

The intensity ratio $I(\frac{1}{2})/I(\frac{3}{2})$ of the two quadrupole lines increases with temperature by $\Delta R=10\pm2\%$ going from 120 to 380°K. These results are in agreement with our calculations ($A=45\%$ and $\Delta R=8.7\%$).

APPENDIX A. ELEMENTS OF THE DYNAMICAL MATRIX

Within the framework of the A-S model, which has been discussed in previous papers,[1–5] the matrix elements corresponding to the first six shells of nearest-neighbor interactions can be constructed from the generators[1]:

$$G(1,1-2)=2(F_{2x}{}^{*}C_z+2F_xC_yC_z),$$
$$G(2,1-1)=2(C_{2y}+2C_xC_y),$$
$$G(3,1-2)=2(2F_{2x}{}^{*}C_{2y}C_z+F_{4x}C_z),$$
$$G(4,1-1)=2C_z,$$
$$G(5,1-2)=4(F_{4x}C_{2y}+F_xC_{3y}+F_{5x}{}^{*}C_y)C_z,$$
$$G(6,1-1)=2(C_{2x}+2C_{3y}C_x),$$

where

$$C_{nx}=\cos nq_x\tfrac{1}{2}a\sqrt{3},\quad C_{ny}=\cos nq_y\tfrac{1}{2}a,$$
$$C_{nz}=\cos nq_z\tfrac{1}{2}c,$$

and

$$F_{nx}=\exp(inq_xa/2\sqrt{3}).$$

Here $n=1$, 2, 3, 4, or 5, and F^* denotes the complex conjugate of F. Following the procedure discussed in previous papers,[8–12] we find the $\alpha\beta$ element of the supermatrix $\mathfrak{D}(\mathbf{q})$ [Eq. (1)] to be

$$\mathbf{D}^{11}=\begin{pmatrix} D_{xx}{}^{11} & D_{xy}{}^{11} & D_{xz}{}^{11} \\ D_{xy}{}^{11} & D_{yy}{}^{11} & D_{yz}{}^{11} \\ D_{xz}{}^{11} & D_{yz}{}^{11} & D_{zz}{}^{11} \end{pmatrix},\quad \mathbf{D}^{12}=\begin{pmatrix} D_{xx}{}^{12} & D_{xy}{}^{12} & D_{xz}{}^{12} \\ D_{xy}{}^{12} & D_{yy}{}^{12} & D_{yz}{}^{12} \\ D_{xz}{}^{12} & D_{yz}{}^{12} & D_{zz}{}^{12} \end{pmatrix},$$

with

$$mD_{xx}{}^{11}=12\delta_1+6\epsilon_{1x}+48\delta_3+6\epsilon_{3x}+168\delta_5+12\epsilon_{5x}+2\beta_{4x}(1-C_{2z})+(3\alpha_2+4\beta_{2x})(1-C_xC_y)+2\beta_{2x}(1-C_{2y})$$
$$+2(\alpha_6+\beta_{6x})(1-C_{2x})+(\alpha_6+4\beta_{6x})(1-C_{3y}C_x),$$

$$mD_{yy}{}^{11}=12\delta_1+6\epsilon_{1x}+48\delta_3+6\epsilon_{3x}+168\delta_5+12\epsilon_{5x}+2\beta_{4x}(1-C_{2z})+2(\alpha_2+\beta_{2x})(1-C_{2y})+(\alpha_2+4\beta_{2x})(1-C_xC_y)$$
$$+(3\alpha_6+4\beta_{6x})(1-C_{3y}C_x)+2\beta_{6x}(1-C_{2x}),$$

$$mD_{zz}{}^{11}=6\epsilon_{1z}+6\epsilon_{3z}+12\epsilon_{5z}+2\beta_{2z}(3-C_{2y}-2C_yC_x)+2\beta_{4z}(1-C_{2z})+2\beta_{6z}(3-C_{2x}-2C_{3y}C_x)+18\gamma^2\delta_1+18\gamma^2\delta_3$$
$$+36\gamma^2\delta_5+2\alpha_4(1-C_{2z}),$$

$$mD_{xy}{}^{11}=\sqrt{3}\alpha_2S_xS_y+\sqrt{3}\alpha_6S_xS_{3y},$$

$$mD_{xz}{}^{11}=mD_{yz}{}^{11}=0,$$

$$-mD_{xx}{}^{12}=4\delta_1[2F_{2x}{}^{*}+F_xC_y]C_z+2\epsilon_{1x}[F_{2x}{}^{*}+2F_xC_y]C_z+16\delta_3[F_{2x}{}^{*}C_{2y}+2F_{4x}]C_z+2\epsilon_{3x}[2F_{2x}{}^{*}C_{2y}+F_{4x}]C_z$$
$$+4\delta_5[16F_{4x}C_{2y}+F_xC_{3y}+25F_{5x}{}^{*}C_y]C_z+4\epsilon_{5x}[F_{4x}C_{2y}+F_xC_{3y}+F_{5x}{}^{*}C_y]C_z,$$

$$-mD_{yy}{}^{12}=12\delta_1[F_xC_yC_z]+2\epsilon_{1x}[F_{2x}{}^{*}+2F_xC_y]C_z+48\delta_3[F_{2x}{}^{*}C_{2y}C_z]+2\epsilon_{3x}[2F_{2x}{}^{*}C_{2y}+F_{4x}]C_z$$
$$+12\delta_5[4F_{4x}C_{2y}+9F_xC_{3y}+F_{5x}{}^{*}C_y]C_z+4\epsilon_{5x}[F_{4x}C_{2y}+F_xC_{3y}+F_{5x}{}^{*}C_y]C_z,$$

$$-mD_{zz}{}^{12}=(6\gamma^2\delta_1+2\epsilon_{1z})[F_{2x}{}^{*}+2F_xC_y]C_z+(6\gamma^2\delta_3+2\epsilon_{3z})[2F_{2x}{}^{*}C_{2y}+F_{4x}]C_z$$
$$+(12\gamma^2\delta_5+4\epsilon_{5z})[F_{4x}C_{2y}+F_xC_{3y}+F_{5x}{}^{*}C_y]C_z,$$

[23] R. M. Housley and R. H. Nussbaum, Bull. Am. Phys. Soc. **9**, 744 (1964).
[24] Walter Kundig, Ken Ando, and Hans Bömmel, Bull. Am. Phys. Soc. **10**, 64 (1965).

$$-mD_{xy}{}^{12}=\frac{12i}{\sqrt{3}}\delta_1F_xS_yC_z-\frac{48i}{\sqrt{3}}\delta_3F_{2x}{}^*S_{2y}C_z+\frac{12i}{\sqrt{3}}\delta_5\{8F_{4x}S_{2y}+3F_xS_{3y}-5F_{5x}{}^*S_y\}C_z,$$

$$-mD_{xz}{}^{12}=-\frac{12i}{\sqrt{3}}\gamma\delta_1\{F_{2x}{}^*-F_xC_y\}S_z-\frac{24i}{\sqrt{3}}\gamma\delta_3\{F_{2x}{}^*C_{2y}-F_{4x}\}S_z+\frac{12i\gamma}{\sqrt{3}}\delta_5\{4F_{4x}C_{2y}+F_xC_{3y}-5F_{5x}{}^*C_y\}S_z,$$

$$-mD_{yz}{}^{12}=-12\gamma\delta_1F_xS_yS_z-24\gamma\delta_3F_{2x}{}^*S_{2y}S_z-12\gamma\delta_5\{2F_{4x}S_{2y}+3F_xS_{3y}+F_{5x}{}^*S_y\}S_z.$$

The S's appearing in these equations denote sine functions whose subscripts have the same meaning as defined for for the C's. The other parameters are

$$\gamma=c/a, \quad \delta_1=K(1,1-2)/(4+3\gamma^2), \quad \epsilon_1=C_B(1,1-2)$$
$$\alpha_2=K(2,1-1), \quad \beta_2=C_B(2,1-1), \quad \delta_3=K(3,1-2)/(16+3\gamma^2), \quad \epsilon_3=C_B(3,1-2)$$
$$\alpha_4=K(4,1-1), \quad \beta_4=C_B(4,1-1), \quad \delta_5=K(5,1-2)/(28+3\gamma^2), \quad \epsilon_5=C_B(5,1-2)$$
$$\alpha_6=K(6,1-1), \quad \beta_6=C_B(6,1-1).$$

In these equations, $K_1(s,\alpha\beta)=C_t(s,\alpha\beta)-C_B(s,\alpha\beta)$, where $C_t(s,\alpha\beta)$ and $C_B(s,\alpha\beta)$ are, respectively, the "bond-stretching" force constant and "bond-bending" force constant for the interaction of the βth atom of the sth shell with the αth atom in the cell at the origin. In the construction of the elements of the D matrix the bond-bending constants occurring in the zz elements are taken to be different from those in the xx elements in order to remove the elastic constraint imposed by the A-S model discussed previously. The specific values of s occurring in the atomic force constants in the previous equations are for magnesium and beryllium.

APPENDIX B. RELATIONS BETWEEN MODIFIED A-S ATOMIC FORCE CONSTANTS AND FOURTH NEIGHBORS FULL TENSOR FORCE MODEL

Equating the elements of the dynamical matrix derived by Collins[10] to those obtained using the modified A-S model we obtain

$$\delta_1=\tfrac{1}{4}[-B_2+B_1], \qquad \alpha_2=\alpha+A_1,$$
$$\epsilon_{1x}=-B_1, \qquad \beta_{2x}=-A_1,$$
$$\epsilon_{1z}=B_3+\tfrac{3}{4}\gamma^2[B_1-B_2], \qquad \beta_{2z}=-A_2,$$
$$\delta_3=\tfrac{1}{16}[-G_2+G_1], \qquad \alpha_4+\beta_{4z}=\delta,$$
$$\epsilon_{3x}=-G_1, \qquad \beta_{4x}=-D_1.$$
$$\epsilon_{3z}=G_3+\frac{3\gamma^2}{16}[G_1-G_2],$$

The constant A_3 appearing in Collins' dynamical matrix must be identically zero. The above notation labeling the neighbors is only appropriate for Mg and Be.

APPENDIX C. A-S MODEL ELASTIC CONSTRAINTS

In this section we derive expressions for the elastic constants for a crystal with two atoms in a unit cell neglecting the optical correction. It is shown that neglecting the relative motion of the two sublattices the symmetry of the A-S model imposes a number of elastic constraints. Elastic constraints for tetragonal and hexagonal lattices are obtained explicitly.

We begin by considering the dynamical matrix in the center-of-mass system. In a previous paper[10] it was shown that the 3×3 matrix corresponding to elastic theory is given by

$$\mathfrak{D}(\mathbf{q})=\mathbf{D}^{11}+\mathrm{Re}\mathbf{D}^{12}-\mathrm{Im}\mathbf{D}^{12}(\mathbf{D}^{11}-\mathrm{Re}\mathbf{D}^{12})\,\mathrm{Im}\mathbf{D}^{12} \quad (\lim\mathbf{q}\to\mathbf{0}). \quad \text{(C.1)}$$

The $\mathbf{D}$ matrices are the supermatrix elements of the A-S dynamical matrix[1] and Re and Im denote the real and imaginary parts. The matrix $(\mathbf{D}^{11}+\mathrm{Re}\mathbf{D}^{12})$ gives the contribution to the elastic properties due to the pure acoustic motion (in phase motion of the two sublattices) and the second term of Eq. (C.1) is a correction due to the relative motion of the two sublattices (referred to as the optical correction).

Let us first determine the form of $\mathbf{D}(\mathbf{q})$ neglecting the effect of the relative motion of the two sublattices (i.e., the optical correction).

Expanding about $q=0$ one obtains

$$\{D^{11}+\mathrm{Re}D^{12}\}_{ij}=\frac{1}{2m}\sum_\beta\sum_n\sum_s\sum_l\sum_m[C_B(S,1\beta)]\delta_{ij}q_lq_mX_l{}^{1\beta}[n(s)]X_m{}^{1\beta}[n(s)]$$
$$+(k(s,1\beta)/\rho_s{}^2)q_lq_mX_i{}^{1\beta}[n(s)]X_j{}^{1\beta}[n(s)]X_m{}^{1\beta}[n(s)]X_l{}^{1\beta}[n(s)]\}, \quad \text{(C.2)}$$

where m is the mass, q_l is the lth Cartesian component of q, $X_l{}^{1\beta}[n(s)]$ is the lth Cartesian component of $R^{1\beta}[n(s)]$ and the remaining symbols are defined in Ref. 1.

The elastic matrix according to continuum theory is

$$\frac{1}{d}\begin{bmatrix} (C_{11}q_x^2+C_{66}q_y^2+C_{44}q_z^2) & (C_{12}+C_{66})q_xq_y & (C_{13}+C_{44})q_xq_z \\ (C_{12}+C_{66})q_xq_y & (C_{66}q_x^2+C_{11}q_y^2+C_{44}q_z^2) & (C_{13}+C_{44})q_yq_z \\ (C_{13}+C_{44})q_xq_z & (C_{13}+C_{44})q_yq_z & C_{44}(q_x^2+q_y^2)+C_{33}q_z^2 \end{bmatrix} \tag{C.3}$$

for a tetragonal crystal where d is the mass density and the C_{ij}'s are elastic constants. The matrix for hexagonal symmetry is obtained from the above by replacing C_{66} by $\frac{1}{2}(C_{11}-C_{12})$. The matrix element in Eq. (C.2) can be expressed as a sum of terms

$$\{D^{11}+\mathrm{Re}D^{12}\}_{ij}=\sum_{l\geq m}\mathcal{E}_{ij}{}^{lm}q_lq_m. \tag{C.4}$$

The $\mathcal{E}_{ij}{}^{lm}$ are then related to the elastic constants occurring in Eq. (C.3). We first note that for any Bravais lattice

$$\mathcal{E}_{ii}{}^{lm}=\frac{1}{2m}\sum_{\beta}\sum_{n}\sum_{s}\left\{C_B(s,1\beta)[X_l{}^{1\beta}]^2+\frac{k(s,1\beta)}{\rho_s{}^2}[X_i{}^{1\beta}]^2[X_l{}^{1\beta}]^2\right\}\delta_{lm} \tag{C.5}$$

and

$$\mathcal{E}_{ij}{}^{lm}=\frac{1}{m}\sum_{\beta}\sum_{n}\sum_{s}\left\{\frac{k(s,1\beta)}{\rho_s{}^2}[X_i{}^{1\beta}]^2[X_j{}^{1\beta}]^2\right\}\delta_{ijlm},\quad i\neq j, \tag{C.6}$$

where δ_{ijlm} is one if the indices are equal in pairs ($i=l$, $j=m$ or $i=m$, $j=l$) but vanishes otherwise. For tetragonal or hexagonal lattices we can make the identification

$$\begin{aligned} &\mathcal{E}_{11}{}^{11}=\mathcal{E}_{22}{}^{22}=C_{11}/d, \\ &\mathcal{E}_{11}{}^{33}=\mathcal{E}_{22}{}^{33}=\mathcal{E}_{33}{}^{11}=\mathcal{E}_{33}{}^{22}=C_{44}/d, \\ &\mathcal{E}_{13}{}^{31}=\mathcal{E}_{32}{}^{32}=\mathcal{E}_{31}{}^{31}=\mathcal{E}_{23}{}^{32}=(C_{13}+C_{44})/d, \\ &\mathcal{E}_{33}{}^{33}=C_{33}/d, \\ &\mathcal{E}_{11}{}^{22}=\mathcal{E}_{22}{}^{11}=\begin{Bmatrix} C_{66}/d \\ (C_{11}-C_{12})/2d \end{Bmatrix}, \\ &\mathcal{E}_{12}{}^{21}=\mathcal{E}_{21}{}^{21}=\begin{Bmatrix} (C_{12}+C_{66})/d \\ (C_{11}+C_{12})/2d \end{Bmatrix}, \end{aligned} \tag{C.7}$$

where we have taken the fourfold (or sixfold) axis along the coordinate axis labeled by 3.

From Eqs. (C.5) and (C.6) and symmetry considerations, it is easily shown that

$$2(\mathcal{E}_{11}{}^{22}-\mathcal{E}_{33}{}^{11})=(\mathcal{E}_{21}{}^{21}-\mathcal{E}_{31}{}^{31}), \tag{C.8}$$

which gives

$$C_{44}-C_{13}-C_{66}+C_{12}=0 \tag{C.9}$$

for tetragonal crystals or

$$3C_{12}+2C_{44}-C_{11}-2C_{13}=0 \tag{C.10}$$

for hexagonal crystals. The optical correction removes these elastic requirements. However, since the optical correction is quite small these elastic requirements must be nearly satisfied. Note that Eqs. (C.9) and (C.10) are independent of the number of neighbors. Using the available elastic data it can be shown that the above constraints are generally not satisfied and, consequently, in order to account for the elastic behavior the A-S model needs to be modified. This is done in the framework of the A-S model by allowing the bond-bending force constants for restoring forces in the basal plane to be different from that normal to the basal plane.